

Two-Body Recombination of NO^+ with NO_2^- and NO_3^- Measured in a Thermal Plasma at 300°K *

P. M. Eisner and M. N. Hirsh

The Dewey Electronics Corporation, Paramus, New Jersey 07652

(Received 29 December 1970)

Two ionic neutralization reactions have been studied with a mass spectrometer and with a planar rf-conductivity probe in the decay of a dilute thermal plasma at 300°K produced by megavolt-electron bombardment of $\text{N}_2:\text{O}_2$ mixtures at 2 to 22 Torr. For $\text{NO}^+ + \text{NO}_2^-$ recombination we obtain a rate coefficient of $(1.75 \pm 0.6) \times 10^{-7} \text{ cm}^3/\text{sec}$, and for $\text{NO}^+ + \text{NO}_3^-$ recombination, $(3.4 \pm 1.2) \times 10^{-8} \text{ cm}^3/\text{sec}$.

Two ionic neutralization reactions, the recombination of NO^+ with NO_2^- and that of NO^+ with NO_3^- , have been studied at 300°K with a mass spectrometer and a planar rf-conductance probe in the decay of a pulsed, dilute thermal plasma in airlike $\text{N}_2:\text{O}_2$ mixtures at 2 to 22 Torr. The measured recombination coefficients concur with recent upper-bound calculations,¹ but not with the merging-beam results of Peterson, Aberth, and Mosely.²

Few measurements of recombination between positive and negative ions have been reported²⁻¹²; prior to the merging-beams measurements,^{2,9-11} the recombining ions were not positively identified. Such meager data have made it difficult to assess the various theoretical approaches to recombination.¹⁰ In previous ion-ion recombination studies in plasmas, two-body recombination is obscured by ionic diffusion in typical laboratory chambers. Mahan and Person⁵ measured a coefficient of $2.1 \times 10^{-7} \text{ cm}^3/\text{sec}$ (without ion identification) for what they believed to be the recombination of NO^+ with NO_2^- , as the low-pressure limit to a pressure-dependent three-body reaction rate. For N_2 as the third body, their data yield a three-body coefficient of $4.0 \times 10^{-9} P \text{ cm}^3/\text{sec}$ for P in Torr. McGowan⁸ has measured ion-ion recombination coefficients in air at pressures above 50 Torr. His value, $2.2 \times 10^{-6} \text{ cm}^3/\text{sec}$ at 1 atm and 25°C , agrees with the earlier work of both Gardner³ and Sayers,⁴ but not with the high-pressure value of Mahan and Person⁵ nor that of Ebert, Booz, and Koepf.¹²

In a merging-ion beam experiment, Peterson, Aberth, and Mosely² obtained recombination coefficients at 300°K of $5.1 \times 10^{-7} \text{ cm}^3/\text{sec}$ for the $\text{NO}^+ + \text{NO}_2^-$ reaction and $5.0 \times 10^{-7} \text{ cm}^3/\text{sec}$ for the $\text{NO}^+ + \text{NO}_3^-$ reaction. Although the merging beam technique¹¹ avoids diffusion and provides ion identification, the ions are epithermal, and results must be extrapolated to 300°K ; also the ions may not be in their ground state.

The experiments described here utilize a large reaction chamber with a fundamental diffusion length Λ of 15.2 cm. The gas is uniformly ionized over its 700-liter volume to minimize further ion loss by diffusion.¹³ Recombining ions should be in thermal equilibrium with the gas since the ion collision frequency with the neutral gas is about $10^8/\text{sec}$ at these pressures while the measured recombination removal frequencies are about 20/sec.

Experimental techniques.—1-MeV electrons irradiate the gas in the cylindrical chamber shown in Fig. 1. Secondary electrons from the primary-electron impact contribute to the total ionization; the gas targets are "thick" for secondaries and "thin" for primaries. The fractional ionization is about 10^{-9} during continuous irradiation^{14,15}; for ion densities encountered in this work, the plasma Debye length is $\leq 0.1 \text{ cm}$. Opposite the foil is an insulated plate used as a planar rf-conductivity probe.

Initially the electron bombardment produces O_2^+ , N_2^+ , O^+ , N^+ , and secondary electrons; the

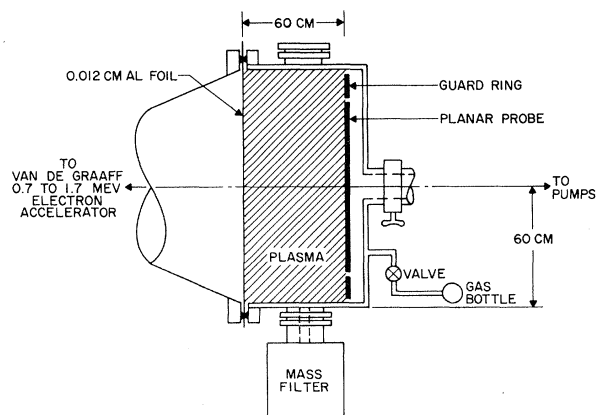


FIG. 1. Schematic representation of reaction chamber and associated equipment. This stainless-steel ultrahigh-vacuum chamber is bakable and contributes less than 1 ppm of impurities to the gas during an experiment.

secondaries rapidly thermalize and attach¹⁴ to O₂, yielding O₂⁻. A series of chemical reactions ensues; after an irradiation of about 30 min, chemical quasiequilibrium is established and NO⁺, NO₂⁻, and NO₃⁻ become and remain the dominant ions. Ion diffusion-loss rates, of the order of 0.1/sec, are small compared to the measured rates for the dominant charge-removal mechanism, ion-ion recombination. A small fraction of the ions does diffuse to the chamber wall, however; some of these effuse through a thin aperture 6.2×10⁻² cm in diameter into a low-pressure region where they are focused and accelerated into the mass spectrometer.

For the recombination measurements, the electron beam is switched repetitively onto the gas for 500 msec, then off for 500 msec. Time-resolved afterglow ion currents are accumulated in a multichannel analyzer; ion counting rates are less than 10⁴/sec. Conductivity measurements are simultaneously made; the 0.1-V/m, 1-kHz rf probing field does not perturb the plasma. Charge density is obtained from the real part of the conductivity σ derived from the Boltzmann equation for an isotropic plasma: Reσ = 1/R = (const)∑_kn_k/m_kν_k, where n_k, m_k, and ν_k are the number density, mass, and effective collision frequency of charge species k. (The applied frequency ω is much smaller than ν_k.)

The mass-spectrometer ion current J_k can be shown¹⁶ to be related to n_k(t) by J_k(t) = S_kn_k(t) × [D_kν_{vk}(t)]^{1/2}, where D_k is the diffusion coefficient (assumed constant for each ion), ν_{vk}(t) is the volume loss frequency, and S_k is a function of aperture geometry, gas pressure, and mass spectrometer efficiency. By definition -n_kν_{vk} = ∂n_k/∂t, so that -n_k∂n_k/∂t = J_k²/D_kS_k²; this Bernoulli-type nonlinear differential equation has the solution

$$n_k(t) = [n_k^2(0) - 2D_k^{-1}S_k^{-2} \int_0^t J_k^2(t) dt]^{1/2}. \quad (1)$$

Results. - From mass spectra obtained under quasiequilibrium conditions, we find that NO⁺ constitutes about 69% of the positive-ion density; NO₂⁻ and NO₃⁻ together constitute about 72% of the negative ions. These fractions change little in the early afterglow (~10 msec). The other ions do not appear to take part in the recombination process, since they decay exponentially. We assume charge equality for the three-ion subsystem throughout the afterglow; the coupled differential equations assumed to govern the afterglow of this subsystem (brackets indicate ion densities)

are¹⁷

$$\begin{aligned} \partial[\text{NO}_2^-]/\partial t &= \alpha_2[\text{NO}_2^-][\text{NO}^+], \\ \partial[\text{NO}_3^-]/\partial t &= \alpha_3[\text{NO}_3^-][\text{NO}^+], \\ \partial[\text{NO}^+]/\partial t &= \partial[\text{NO}_2^-]/\partial t + \partial[\text{NO}_3^-]/\partial t. \end{aligned} \quad (2)$$

Figure 2 shows the NO⁺, NO₂⁻, and NO₃⁻ mass-spectrometer currents in the afterglow at 4.3 Torr and the ion densities calculated from them using (1). Six constants, two for each ion, are needed to obtain the ion densities; from the derived densities, the ion-ion recombination coefficients α₂ and α₃ are calculated. The constants are deduced from a computational fit constrained by two criteria: Charge equality should hold throughout the afterglow, and the resulting initial loss rate for NO⁺ should be related to the previously measured total positive-ion produc-

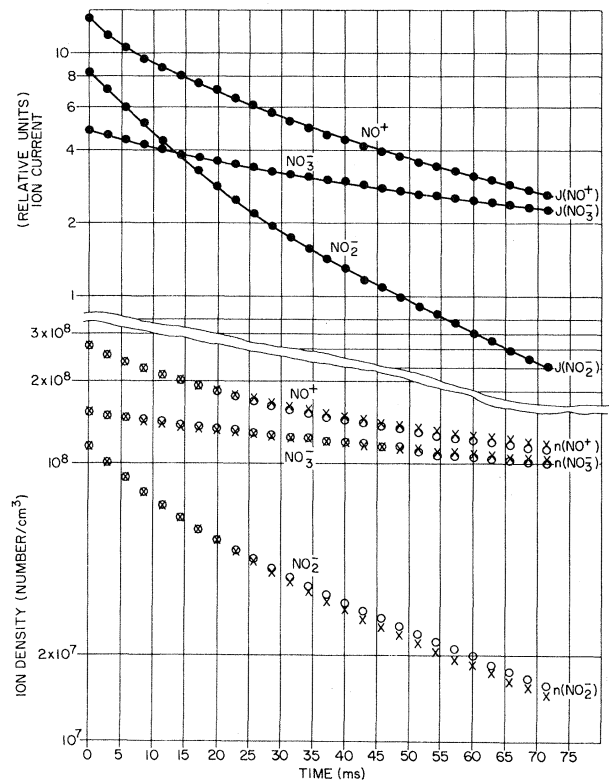


FIG. 2. Mass-spectrometer ion currents versus time in the afterglow are shown at the top of the figure; the solid curves were drawn through 75 data-channel points from the multichannel analyzer. The points on these curves show the 26 times at which the data were digitized for further analysis. Circles in the lower part of the figure indicate the densities computed from the data as described in the text; crosses show the reconstructed afterglow densities computed from the rate equations.

tion rates¹⁴ by

$$\begin{aligned} \partial[\text{NO}^+]/\partial t|_{t=0} &= 0.69KPj \\ &= 7.18 \times 10^9 \text{ cm}^{-3} \text{ sec}^{-1}, \end{aligned} \quad (3)$$

where 0.69 is the ratio of NO^+ to total positive-ion density, K is a constant, and j is the electron beam flux. At 26 points in the afterglow, ion densities, loss frequencies, and α_2 and α_3 are calculated for various sets of the six constants. Loss frequencies are obtained from the derived densities by a six-point finite-difference scheme. The best fit (shown in Fig. 2) satisfies charge equality to better than 5% throughout the afterglow, yields a calculated value for (3) of $7.05 \times 10^9 \text{ cm}^3/\text{sec}$, and produces recombination coefficients from (2) which are constant to within 15% throughout the measured afterglow. The average values obtained are $\alpha_2 = 1.75 \times 10^{-7} \text{ cm}^3/\text{sec}$ and $\alpha_3 = 3.4 \times 10^{-8} \text{ cm}^3/\text{sec}$. Figure 2 includes ion-density afterglows reconstructed from the rate equations (2) with the recombination coefficients and initial ion densities computed from the data. The agreement between the density decays computed directly from the data and those reconstructed from (2) corroborates our interpretation of these data.¹⁸

The time-varying plasma resistance in the afterglow (Fig. 3), $R(P, t) = R(P, 0) + f(P)t$, yields total ion densities having the form of the recombination-controlled afterglow: $1/n(t) = 1/n(0)$

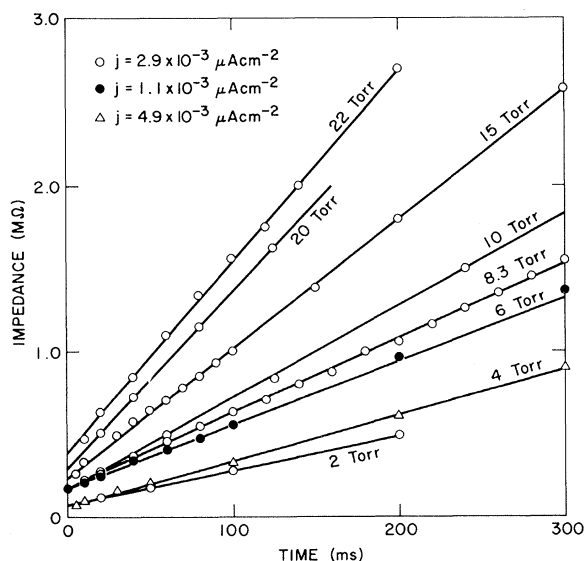


FIG. 3. Real part of plasma impedance versus time in the afterglow for a range of pressures and electron beam fluxes. Straight lines drawn through the data points indicate ionic-recombination control of plasma density.

$+ \alpha t$. For a single positive ion, NO^+ , we have $R^{-1}(0)\partial R(t)/\partial t = G = \alpha[\text{NO}^+]$ at $t=0$, where α is the effective NO^+ recombination rate. Since $\partial[\text{NO}^+]/\partial t = \alpha[\text{NO}^+]^2$, then $\alpha = G^2/KPj$. Between 15 and 22 Torr, $\alpha = (4.0 \pm 1.0) \times 10^{-8} \text{ cm}^3/\text{sec}$, in agreement with the 4.3-Torr mass-spectrometer result for the $\text{NO}^+, \text{NO}_3^-$ recombination; this indicates that three-body contributions to this reaction are small at pressures up to 22 Torr. At lower pressures, the effective recombination coefficients increase with decreasing pressure. At 2 Torr, where NO_2^- dominates the negative-ion spectrum, the effective rate coefficient from the conductivity data, $(2.2 \pm 0.4) \times 10^{-7} \text{ cm}^3/\text{sec}$, is close to the mass-spectrometer result for α_2 . Computed diffusion-loss rates are less than 5% of the recombination-loss rates for the afterglows in Fig. 3.

Conclusion.—We have measured ion-ion recombination-rate coefficients for two important ionospheric reactions¹⁹ at thermal energies, $\text{NO}^+ + \text{NO}_2^- \rightarrow \text{neutrals}$, and $\text{NO}^+ + \text{NO}_3^- \rightarrow \text{neutrals}$, using two complementary techniques. The conductivity measurements extend the detailed mass-spectrometer results, obtained at one pressure, over the entire pressure range studied, 2 to 22 Torr.

Major sources of error are a 30% uncertainty in the NO^+ production rate and a 20% error for data-fitting uncertainties and contributions from competing processes.¹⁸ For three-body contributions to the rates, the results of Mahan and Person⁵ indicate a value of $2 \times 10^{-8} \text{ cm}^3/\text{sec}$ for α_2 at 4.3 Torr; our result is consistent with this. We see no evidence for a three-body contribution to α_3 up to 22 Torr; thus it is probably less than $5 \times 10^{-10} P \text{ cm}^3/\text{sec}$ (P in Torr).

The final results and estimated errors are

$$\alpha_2(\text{NO}^+ + \text{NO}_2^-) = (1.75 \pm 0.6) \times 10^{-7} \text{ cm}^3/\text{sec};$$

$$\alpha_3(\text{NO}^+ + \text{NO}_3^-) = (3.4 \pm 1.2) \times 10^{-8} \text{ cm}^3/\text{sec}.$$

They agree with Olson's calculations,¹ $\alpha_2 \leq (1.6 \pm 0.4) \times 10^{-7} \text{ cm}^3/\text{sec}$ and $\alpha_3 \leq (13 \pm 5) \times 10^{-8} \text{ cm}^3/\text{sec}$; α_2 agrees with the experimental results of Mahan and Person⁵ as well. The considerable discrepancy between our results and those of Peterson, Aberth, and Mosely² may indicate vibrational or electronic excitation in their merging ion beams.

The authors wish to thank Eliaz Poss for his aid in data collection, David Maerz for his assistance throughout the experiment, and Dr. A. V. Phelps for his assistance with the ion-sam-

pling theory.

*Work supported by Defense Atomic Support Agency, under NWER Subtask HC010, Contract No. DASA-01-70-C-0032.

¹R. E. Olson, "Absorbing-Sphere Model for Calculating Thermal Energy Ion-Ion Recombination Reaction Rates" (to be published); R. E. Olson, J. R. Peterson, and J. Mosely, *J. Chem. Phys.* **53**, 3391 (1970).

²J. R. Peterson, W. Aberth, and J. Mosely, to be published; J. Mosely, W. Aberth, and J. R. Peterson, "Ion-Ion Mutual Neutralization Cross Sections for O_2^+ + NO_3^- and NO^+ + NO_3^- ," in Proceedings of the 23rd Annual Gaseous Electronics Conference, Hartford, Conn., October 1970 (to be published).

³M. E. Gardner, *Phys. Rev.* **53**, 75 (1938).

⁴J. Sayers, *Proc. Roy. Soc., Ser. A* **169**, 83 (1938).

⁵B. H. Mahan and J. C. Person, *J. Chem. Phys.* **40**, 392 (1964).

⁶T. S. Carlton and B. H. Mahan, *J. Chem. Phys.* **40**, 3683 (1964).

⁷H. Y. Yeung, *Proc. Phys. Soc., London* **71**, 341 (1958).

⁸S. McGowan, *Can. J. Phys.* **45**, 439 (1967).

⁹W. H. Aberth and J. R. Peterson, *Phys. Rev. A* **1**, 158 (1970).

¹⁰R. D. Rundel, K. L. Aitken, and M. F. A. Harrison, *J. Phys. B: Proc. Phys. Soc., London* **2**, 954 (1969).

¹¹W. Aberth, J. R. Peterson, D. C. Lorents, and C. J. Cook, *Phys. Rev. Lett.* **20**, 979 (1968); J. Mosely, W. Aberth, and J. R. Peterson, *Phys. Rev. Lett.* **24**,

435 (1970).

¹²H. G. Ebert, J. Booz, and R. Koeppe, *Z. Phys.* **181**, 187 (1964).

¹³M. N. Hirsh, P. N. Eisner, and J. A. Slevin, *Rev. Sci. Instrum.* **39**, 1547 (1968).

¹⁴M. N. Hirsh, P. N. Eisner, and J. A. Slevin, *Phys. Rev.* **178**, 175 (1969).

¹⁵M. N. Hirsh, E. Poss, and P. N. Eisner, *Phys. Rev. A* **1**, 1615 (1970).

¹⁶This relation assumes that recombination is the only volume loss process and that diffusion controls the ion densities in the immediate vicinity of the chamber walls, and hence controls the mass-spectrometer currents. This model, described in a forthcoming paper, agrees closely with rigorous calculations [E. P. Gray and D. E. Kerr, *Ann. Phys. (New York)* **17**, 276 (1962)] for the case of a single-positive, single-negative-ion plasma under these experimental conditions.

¹⁷Although the NO^+ -electron recombination coefficient [C. S. Weller and M. A. Biondi, *Phys. Rev.* **172**, 198 (1968)] is about the same as the NO^+ -ion recombination coefficient, electrons can be neglected because their density during irradiation, about $7 \times 10^6 \text{ cm}^{-3}$, is two decades below that of the ions, and in the afterglow it decreases more rapidly than the ions (see Ref. 14).

¹⁸Negative-ion reactions with neutral NO , O_3 , and NO_2 have been suggested [N. G. Adams *et al.*, *J. Chem. Phys.* **52**, 3133 (1970)] which could couple the NO_2^- and NO_3^- densities. We see no gross effects attributable to these reactions.

¹⁹R. E. LeVier and L. M. Branscomb, *J. Geophys. Res.* **73**, 27 (1968).

Ground-State Energy of a Charged-Boson Gas

Deok Kyo Lee

Department of Physics and Astronomy, University of Kansas, Lawrence, Kansas 66044

(Received 1 March 1971)

The ground-state energy of a charged-boson gas at high density is re-examined and it is found that Brueckner's exact result for the second-order energy is reproduced precisely by Feenberg's variation-perturbation method.

In recent years the charged-boson gas has been an interesting subject in the theoretical study of many-body boson problems. The ground-state energy of the system at high density was first evaluated exactly to second order by Brueckner,¹ who carried out complete summations of one- and two-ring diagrams using the Bogoliubov theory; his exact result is²

$$E/N = -0.8031/r_s^{3/4} + 0.0280 + O(r_s^{3/4}), \quad (1)$$

which agrees *numerically* with the variational result obtained by Lee and Feenberg³ in the Bijl-Dingle-Jastrow (BDJ) wave-function space. Because of this numerical agreement considerable energy has been expended in attempts to prove that two results agree analytically. The purpose of this report is to clarify this point by showing that the variational energy is higher in second order than the exact energy by an amount exactly equal to the energy shift generated by the three-phonon vertex.⁴

In order to evaluate the difference between the exact and variational energies in second order, here we introduce

$$t = \frac{1}{\sqrt{2}} \left[\frac{\hbar^2}{4\pi m e^2 \rho} \right]^{1/4} k, \quad \bar{t}'' = \bar{t} - \bar{t}', \quad \omega = [1 + t^4]^{1/2}, \quad S = t^2/\omega, \quad \{f\} = f + f' + f'' = f(t) + f(t') + f(t''). \quad (2)$$